



Universiteit
Leiden
The Netherlands

Solitary Waves and Fluctuations in Fragile Matter

Upadhyaya, N.

Citation

Upadhyaya, N. (2013, November 5). *Solitary Waves and Fluctuations in Fragile Matter*. *Casimir PhD Series*. Retrieved from <https://hdl.handle.net/1887/22138>

Version: Not Applicable (or Unknown)

License: [Leiden University Non-exclusive license](#)

Downloaded from: <https://hdl.handle.net/1887/22138>

Note: To cite this publication please use the final published version (if applicable).

Cover Page



Universiteit Leiden



The handle <http://hdl.handle.net/1887/22138> holds various files of this Leiden University dissertation.

Author: Upadhyaya, Nitin

Title: Solitary waves and fluctuations in fragile matter

Issue Date: 2013-11-05

GRANULAR INTERFACES

In this chapter, we start with the two dimensional problem of determining the reflection and transmission of a strongly non-linear solitary wave-front incident upon an interface between two hexagonal lattices both in a sonic vacuum (zero sound speed), but with different particle masses specified by the ratio $A = m_2/m_1$. We treat the solitary wave as a quasi-particle with an effective mass and model the interaction with a two-dimensional granular interface, as an elastic collision process conserving energy and linear momentum that is validated by simulations. Here, two distinct scenarios emerge valid approximately for - (a) $A \sim 1$ and (b) $A \ll 1$.

In the case $A \sim 1$, the incident solitary waves evolves into two new solitary waves, a leading one that is transmitted into the lighter medium and a smaller one, that is either reflected or transmitted depending upon the mass ratio being greater or less than 1. This is simply modelled as an elastic disintegration of a solitary wave. In the $A \ll 1$ case, the solitary waves moves from a much denser medium to a lighter medium and it is seen that the last row of "heavy" beads at the interface, absorbs on a "fast" time scale the main part of the energy and linear momentum of the incident solitary wave-front (assumed parallel to the interface) and detaches from the heavy medium while repeatedly colliding with the the lighter medium, see Fig. (2.1) (c). Through this process, the last row decelerates on a "slower" time scale, and generates a train of asymptotically well separated solitary waves in the "lighter" sonic vacuum. Crucial to understanding this phenomenon is the role of contact breaking at the interface and the resulting break-down of the continuum approximation that we model using an elastic collision process between the heavy beads and the solitary wave quasi-particle.

We then apply our understanding from the study of parallel interfaces, to study how a solitary wave that is incident at an angle to the interface, moves from one medium to another. Here, we find that the angles of refraction and reflection of the the leading solitary waves that are generated as a result of the elastic disintegration, are surprisingly well captured by a granular

analogue of Snell's law that holds irrespective of the solitary wave-front amplitude, for small angles of incidence.

2.1 SIMULATIONS

In order to investigate the solitary wave scattering at a two dimensional granular interface, we perform molecular dynamics simulations for a hexagonal packing of 10^4 frictionless spherical grains, using periodic boundary conditions. As shown in Fig. (2.1), an interface is introduced by assigning a mass m_1 to the rows of grains on its left (shown in red) and a mass m_2 to rows on its right (shown in yellow). Both portions of the hexagonal lattice are comprised of grains with zero initial overlap and equal diameters. Two grains of radius R and masses $\{m_i, m_j\}$ at positions $\{\vec{x}_i, \vec{x}_j\}$ interact via a one-sided non-linear repulsive potential following Hertz law [5]

$$V_{ij} = \frac{K_{ij}}{\alpha} \delta_{ij}^{\frac{5}{2}} \quad (2.1)$$

only for positive compressional strains $\delta_{ij} \equiv 2R - |\vec{x}_i - \vec{x}_j| > 0$, otherwise $V_{ij} = 0$, when $\delta_{ij} \leq 0$. Here, the interaction parameter $K_{ij} = \frac{2}{3}RE_{ij}^*$ is expressed in terms of the effective Young's modulus of the two particles, E_{ij}^* , see Ref. [20] for more details. Consequently, due to the non-linear interaction potential and absence of any initial overlap between grains, both the hexagonal lattices are in a state of sonic vacuum. At $t = 0$, we impart to the left-most row a speed u_p and subsequently integrate Newton's equations of motion numerically subject to periodic boundary conditions perpendicularly to the direction of propagation. As seen in Fig. (2.1) (a), we see a well defined solitary wave that propagates along the direction of impact.

2.2 QUASI-PARTICLE MODEL

We take advantage of the isotropic elasticity of the hexagonal lattice to assume that the dynamics of a solitary wave-front parallel to the interface, as in Fig. (2.1), is effectively one dimensional and governed, in the continuum limit, by the non-linear wave equation Eq. (A.10):

$$\xi_{tt} = c^2 \left[\xi^{\frac{3}{2}} + \frac{2R^2}{5} \xi^{\frac{1}{4}} (\xi^{\frac{5}{4}})_{xx} \right]_{xx}, \quad (2.2)$$

where c is a material constant and $\xi(x, t)$ is the strain field $\xi(x, t) = -\partial_x u(x, t)$ expressed in terms of the particle displace-

ment field, $u(x, t)$, along the x direction. The left-hand side of Eq. (2.2) is the standard inertia term, the second term on the right-hand side captures non-linear dispersive effects, while the first arises from the restoring force as in the wave-equation, if one considers that the force is not linear, but it depends on $\xi^{3/2}$ according to Hertz law.

As discussed in the previous chapter, a strongly nonlinear solitary wave solution of Eq. (2.2) can be derived analytically [6] and it has been validated by extensive simulations and experiments mostly on granular chains [15, 6, 23, 24, 17, 33, 26, 27]. Crucially, the total energy $E = \frac{p^2}{2m_{\text{eff}}}$ carried by the solitary wave depends quadratically on its total momentum P , which allows the interpretation of the solitary wave as a quasi-particle with an effective mass $m_{\text{eff}} \approx 1.4m$. We next use this quasi-particle interpretation of the solitary wave to study its interaction with a two dimensional granular interface.

2.3 WEAK DISORDER

If the ratio of bead masses on either side of the interface $A = \frac{m_2}{m_1}$ is nearly equal to 1, an initial solitary wave excitation is seen to split at the interface into two new solitary waves: a leading solitary wave that crosses the interface into the new medium and a smaller solitary wave, that is either reflected back or transmitted depending on the mass ratio being greater or less than one. The quasi-particle notion of the solitary wave provides a simplified model to study the interaction of the solitary wave with the granular interface as an elastic collision process (conserving momentum and energy) resulting in the disintegration of the initial solitary wave into two new solitary waves [17, 39]

$$P_0 = P_1 + P_2, \quad (2.3)$$

$$\frac{p_0^2}{2m_{1,\text{eff}}} = \frac{p_1^2}{2m_{1,\text{eff}}} + \frac{p_2^2}{2m_{2,\text{eff}}} \quad (2.4)$$

where, P_0 is the momentum of the incident solitary wave, P_1 is the momentum of the smaller reflected or transmitted solitary wave and P_2 is the momentum of the leading transmitted solitary wave. Solving, we obtain

$$P_1 = \frac{P_0 (1 - A)}{(1 + A)}, \quad (2.5)$$

where $A \equiv \frac{m_{2,\text{eff}}}{m_{1,\text{eff}}}$ and

$$P_2 = \frac{2P_0}{1+A}. \quad (2.6)$$

The predicted momentum P_1, P_2 are found to be in good agreement with numerical data in both one and two dimensional granular interfaces for $A \sim 1$ [17, 39]. Since this case is well studied and we will make further use of it in a later chapter where the validity of this result will be explicitly used (Chapter 3), we now turn to discussing the more novel observations when the mass ratio $A \ll 1$.

2.4 STRONG DISORDER : $A \ll 1$

As shown in Fig. (2.1)(a), the initial impulse imparted to the left most beads, leads to the generation of a non-linear wave front parallel to the interface that travels towards the right with a speed $V_s \sim u_p^{1/5}$ analogously to solitary waves in granular chains [6]. At t_0 , all the energy and linear momentum P_0 of the incident solitary wave is concentrated in the ‘‘heavy’’ (red) chain of beads and we have an undisturbed chain of ‘‘light’’ (yellow) beads. At later times, shown in Fig. (2.1)(b), when the solitary wave has interacted with the interface, we see a ruptured interface with one of the inter-facial rows of heavy (red) beads ‘‘dancing’’ in contact with the lattice of lighter (yellow) beads, throttling the generation of an oscillatory wave profile in the lighter lattice close to the interface. This oscillatory wave is subsequently disintegrated into a sequence of separate solitary waves, as shown in Fig. (2.1)(c). The separate solitary waves propagate with different speeds (dependent on their amplitude), while a second collision of the ‘‘dancing’’ interfacial row of particles, shown in Fig. (2.1)(d), generates a second delayed solitary-wave train with smaller amplitudes.

The notion of the solitary wave as a quasi-particle again allows us to construct a simple quasi one-dimensional model for the generation of the solitary wave train, illustrated schematically in Fig. (2.2). At t_0 , we assume that a chain of *light* yellow beads is uncompressed and all the energy and linear momentum P_0 , carried by the incident solitary wave, is concentrated in the *heavy* red interfacial particle. At a subsequent time t_1 a single solitary wave is generated in the *light* chain by reducing the energy and linear momentum of the interfacial heavy particle. We apply conservation of energy and linear momen-

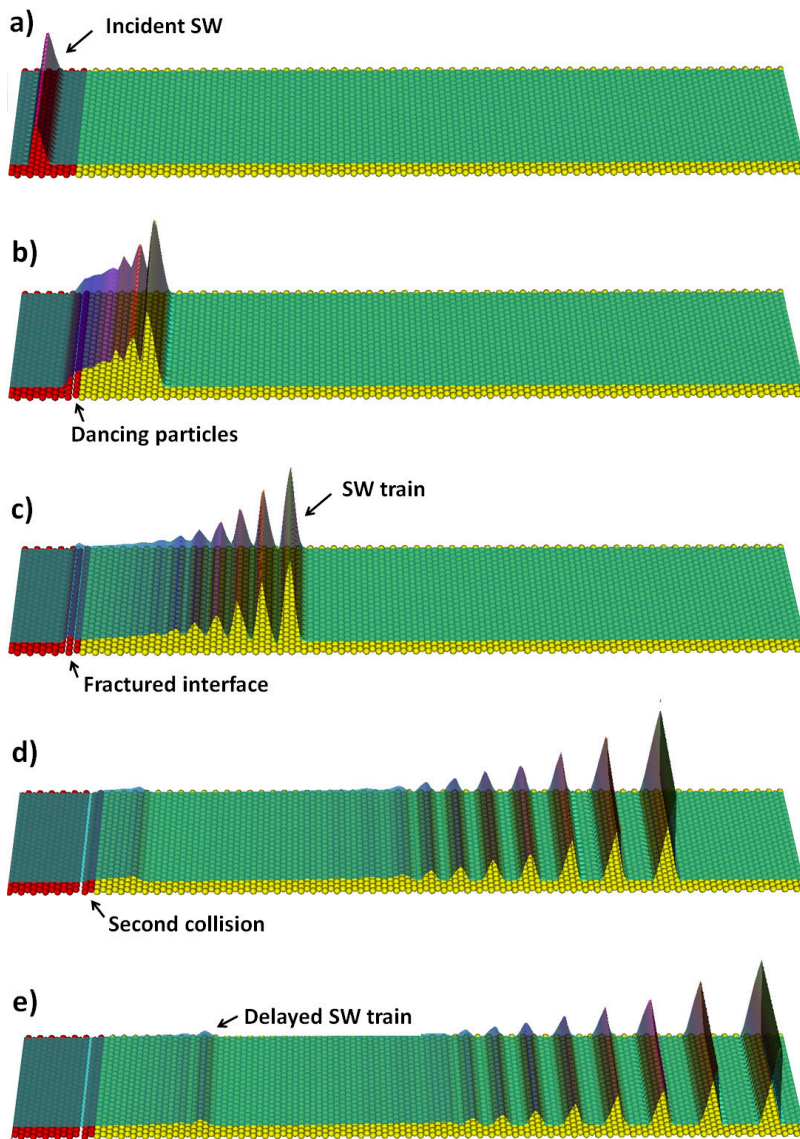


Figure 2.1: Time sequence leading to the generation of a solitary wave train in simulations. The (red) beads on the left of the interface constitute the heavier medium with mass m_1 and the (yellow) beads on the right of the interface constitute the lighter medium with mass m_2 . The mass ratio $\Lambda \equiv \frac{m_2}{m_1} = 0.125$. The velocity field overlayed in green, denotes the instantaneous speeds of the beads.

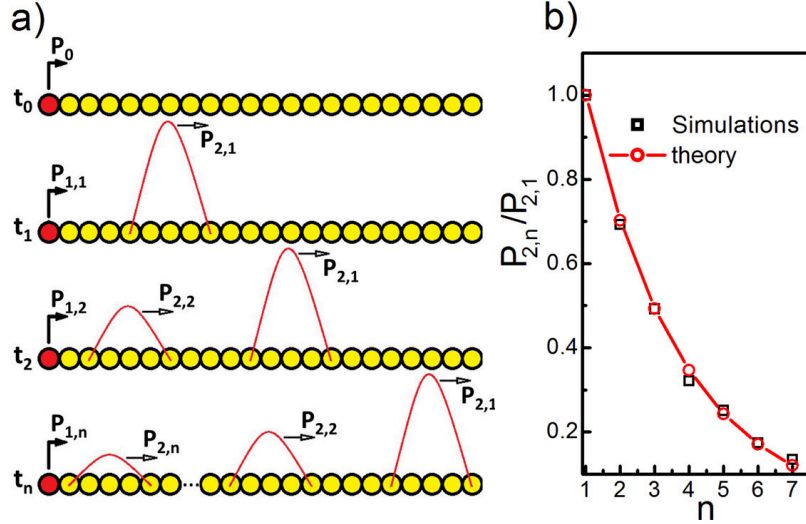


Figure 2.2: (a) Schematic illustration of our model for the formation of a solitary-wave train, side-view. (b) Momentum ratios $\frac{P_{2,n}}{P_{2,1}}$ between the n -th solitary wave and the leading one in the train for $A = \frac{m_2}{m_1} = 0.125$. Red circles are the theoretical predictions while the black squares are the numerical values from the simulations of Fig. (2.1).

tum to the collision process between the “dancing” bead with mass m_1 and the solitary wave, treated as a quasiparticle with mass $m_{2,\text{eff}}$. Note, it is here that the effective mass of the solitary wave becomes crucial to our understanding of the process, unlike the case for $A \sim 1$, where the collision is between two solitary waves with effective masses that are rescaled by the same constant value (≈ 1.4) and thus cancel out. We calculate the momentum of the “dancing” interfacial particle $P_{1,1}$ after the first collision as

$$P_{1,1} = \frac{P_0 (B - 1)}{(B + 1)}, \quad (2.7)$$

where $B \equiv \frac{m_1}{m_{2,\text{eff}}}$. The momentum $P_{2,1}$ carried by the first leading solitary wave at $t = t_1$ is

$$P_{2,1} = \frac{2P_0}{B + 1}. \quad (2.8)$$

At time t_2 another independent single solitary wave is generated in the “light” chain, further reducing the energy and linear momentum of the “dancing” interfacial particle. Upon applying conservation of energy and linear momentum, as before, and assuming that the first solitary wave does not participate

in this process, we find the momentum of the “dancing” particle at $t = t_2$, $P_{1,2}$, and of the second solitary wave, $P_{2,2}$, as

$$P_{1,2} = \frac{P_0 (B - 1)^2}{(B + 1)^2}, P_{2,2} = \frac{2P_0 (B - 1)}{(B + 1)^2}. \quad (2.9)$$

Upon iterating this process n times (assuming that the generation of each solitary wave occurs independently and does not interfere with the previous or subsequent solitary wave), we find that the “heavy” interfacial bead at $t = t_n$ is left with a linear momentum $P_{1,n}$ while the n -th solitary wave carries momentum $P_{2,n}$ given by

$$P_{1,n} = \frac{P_0 (B - 1)^n}{(B + 1)^n}, P_{2,n} = \frac{2P_0 (B - 1)^{n-1}}{(B + 1)^n}. \quad (2.10)$$

Fig. (2.2)(b) illustrates the favorable comparison of $\frac{P_{2,n}}{P_{2,1}} = \left(\frac{B-1}{B+1}\right)^{n-1}$ against numerical data (red circles) for $A = 0.125$. The amplitudes of the delayed secondary sequence of solitary waves generated is neglected in our approximate model.

DISORDERED PACKINGS

In the previous chapter we found that approximating the solitary wave as quasi-particle, provides us with a simple model to study its interaction with an isolated granular interface characterized by mass mismatch. Upon crossing the interface, the solitary wave was seen to disintegrate into approximately two solitary waves when the mass ratio is small. This suggests that if we keep track of the leading transmitted solitary wave as it propagates through a series of well separated interfaces as a model for a medium with mass disorder, we will find the solitary wave amplitude to decrease with distance.

In this chapter, we study numerically and analytically the decay of the solitary wave excitations in such a two dimensional mass disordered and amorphous packings of grains that are just in contact with their nearest neighbours. We find that there is a regime of weak mass disorder, where the solitary wave excitation generated in response to an impulse decays exponentially at early times, with a rate that depends upon the amount of disorder. In the long time limit, the initially well defined solitary wave soon transitions into a triangular shock like profile, whose amplitude decays as a power law with an exponent that is consistent with $\frac{1}{2}$ and independent of the amount of disorder. Additionally, there is a regime of strong disorder where the quasi-particle model is not adequate to model the interaction of the solitary waves with the material inhomogeneities. Rather in this regime, the power law decay is the dominant mechanism of attenuation and we observe this in hexagonal lattices with strong mass disorder (large variance in masses) as well as in jammed amorphous packings close to their critical packing fraction*.

* The research ideas presented in this chapter evolved out of discussions with L. R. Gomez and V. Vitelli and are part of Reference[45]. Thanks to L.R. Gomez for the 2D simulations and accompanying figure 3.3.

